



ACADEMIC
PRESS

Biochemical and Biophysical Research Communications 294 (2002) 184–190

BBRC

www.academicpress.com

Domain-swapped structure of a mutant of cyanovirin-N[☆]

Istvan Botos,^a Toshiyuki Mori,^b Laura K. Cartner,^c Michael R. Boyd,^{b,1}
and Alexander Wlodawer^{a,*}

^a Macromolecular Crystallography Laboratory, National Cancer Institute at Frederick, Frederick, MD 21702-1201, USA

^b Molecular Targets Drug Discovery Program, Center for Cancer Research, National Cancer Institute at Frederick, Frederick, MD 21702-1201, USA

^c Science Applications International Corporation at Frederick, NCI-Frederick, Frederick, MD 21702-1201, USA

Received 3 May 2002

Abstract

Cyanovirin-N (CV-N) is a potent 11 kDa HIV-inactivating protein that binds with high affinity to the HIV surface envelope protein gp120. A double mutant P51S/S52P of CV-N was engineered by swapping two critical hinge-region residues Pro51 and Ser52. This mutant has biochemical and biophysical characteristics equivalent to the wild-type CV-N and its structure resembles that of wild-type CV-N. However, the mutant shows a different orientation in the hinge region that connects two domains of the protein. The observation that this double mutant crystallizes under a wide variety of conditions challenges some of the current hypotheses on domain swapping and on the role of hinge-region proline residues in domain orientation. The current structure contributes to the understanding of domain swapping in cyanovirins, permitting rational design of domain-swapped CV-N mutants. © 2002 Published by Elsevier Science (USA).

Cyanovirin-N (CV-N), initially isolated from cultures of the cyanobacterium (blue-green algae) *Nostoc ellipsosporum* [1], is a natural product capable of preventing HIV infection [2] and provides a potential new lead for the design of drugs against AIDS. CV-N is a highly potent virucidal protein, low nanomolar concentrations of which inactivate diverse T-tropic, M-tropic and dual-tropic primary isolates of HIV-1, HIV-2, SIV, and FIV [1] and certain other enveloped viruses [3]. CV-N also inhibits in vitro fusion of HIV-infected and non-infected cells and cell-to-cell transmission of HIV-1 infection [1].

The anti-HIV activity of CV-N is mediated through high-affinity interactions with the viral surface envelope glycoprotein gp120 [1] and by blocking essential interactions of gp120 with receptors on various target cells [4,5]. CV-N binds to the envelope protein through unique interactions with the high-mannose oligosaccharides oligomannose-8 and -9 present in both glycoproteins [6,7]. The ability of CV-N to distinguish between high-mannose and complex oligosaccharides may account for the specificity of binding of CV-N to gp120 [7]. However, results based on thermodynamic analysis show that in addition to the interactions with specific oligosaccharides, discrete protein–protein interactions might play an important ancillary role in the CV-N/gp120 binding [7].

CV-N is a 11 kDa protein (101 amino acids) that exhibits less than 20% homology to any other known protein. A series of mutants and variants were engineered for CV-N [8] and the availability of the three-dimensional structures of CV-N obtained by both NMR and crystallography [9,10] facilitated the design of key mutations, capable of altering some of the characteristics of the protein. CV-N contains two consecutive domains similar in sequence and almost identical in structure that form either a single compact molecule

[☆] Abbreviations: CV-N, cyanovirin-N; P51S/S52P, CV-N mutant; HIV-1, human immunodeficiency virus Type 1; HIV-2, human immunodeficiency virus Type 2; SIV, simian immunodeficiency virus; FIV, feline immunodeficiency virus; sgp120, soluble HIV envelope glycoprotein; ELISA, enzyme-linked immunosorbent assay; PBS, phosphate-buffered saline; TPBA, phosphate-buffered saline augmented with 0.05% Tween 20; XTT, 2,3-bis[2-methoxy-4-nitro-5-sulfophenyl]-2H-tetrazolium-5-carboanilide inner salt; PCMBs, *para*-chloro-mercuribenzenesulfonate; r.m.s.d., root mean square deviation.

* Corresponding author. Fax: +1-301-846-6128.

E-mail address: wlodawer@ncifcrf.gov (A. Wlodawer).

¹ Present address: College of Medicine, USA Cancer Research Institute, University of South Alabama, Mobile, AL 36688, USA.

observed in most of the NMR structures or a domain-swapped dimer that was reported for all crystal structures of this protein.

Mutations in the hinge region of CV-N can influence the dynamics of the two domains, preventing three-dimensional domain swapping or locking the protein in an extended conformation. Three-dimensional domain swapping is an oligomerization process where two or more protein chains exchange identical domains [11]. Mechanisms and evolutionary aspects of domain swapping have been analyzed in detail [12]. The term “three-dimensional” distinguishes the intertwining of protein chains in their structures from the common term “domain swapping” used to describe the genetic reengineering of proteins. A reciprocal exchange of domains leads to dimers, a non-reciprocal one to oligomers [13].

The monomeric form of CV-N is predominant in solution but the dimer can be obtained by purification or during crystallization. Previous results [9,14,15] led to a hypothesis that domain swapping is the result of high protein concentrations at low pH. Recently obtained data show that purified CV-N at low pH is a mixture of 70:25:5 monomer:dimer:oligomer [16], while upon titration to pH > 5.0, the dimer fraction falls to 5–10% [9].

A hinge-region S52P mutant of CV-N, in which Ser52 was replaced with a proline, was discovered in a screen of a phage-displayed mutant CV-N library; it has been shown that this mutant exists exclusively as a stable dimer in solution [17]. In addition, S52P was somewhat less potent against HIV, compared to the wild-type CV-N. Subsequently, another CV-N mutant, P51G, was designed; this mutant is mainly monomeric in solution with only a trace amount of dimer and, under certain experimental conditions, was significantly more stable than wild-type CV-N [18].

Since it is clear that the nature of both of the hinge-region residues 51 and 52 strongly affects the properties of CV-N, we decided to investigate a double mutant, P51S/S52P, in which these two critical residues were swapped in their sequence. Results of such mutations aimed at the investigation of the interdomain hinge region of CV-N are described below.

Materials and methods

Strains and materials. Restriction endonucleases were obtained from Amersham Pharmacia Biotech (Piscataway, NJ). *Pfu* Turbo DNA polymerase was from Stratagene (La Jolla, CA). All other chemicals were of analytical grade.

Construction of expression vectors for P51S/S52P in *Escherichia coli* and purification of the corresponding recombinant proteins. The wild-type CV-N was expressed and purified as described elsewhere [19]. The QuikChange Site-Directed Mutagenesis Kit from Stratagene (La Jolla, CA), with specific oligo-DNA primer sets, was utilized to replace Pro at position 51 of CV-N with Ser and Ser at position 52 of CV-N with Pro (P51S/S52P). After all the sequences were verified by DNA sequencing, the expression of the recombinant proteins was induced with

1.0 mM IPTG in transformed *E. coli* BL21 (DE3) cells (Novagen, Madison, WI) and periplasmic extracts were prepared by an osmotic-shock method as described previously [19]. The expressed proteins from the periplasma were purified by reverse-phase liquid chromatography as described [19]. Molecular mass and purity of CV-N were confirmed by electrospray ionization mass spectrometry and the protein concentrations were determined by amino acid analysis.

ELISA study for *sgp120* binding of CV-N mutants. ELISA was performed to compare binding activities of the CV-N mutant proteins to soluble *gp120* (*sgp120*). Ninety-six-well assay plates (Nalge Nunc International, Naperville, IL) were coated for 3 h at 37 °C with 50 ng/100 µl/well of *sgp120* in PBS and non-specific binding sites were blocked with 200 µl of 5% non-fat dry milk (w/v) in PBS overnight at 4 °C, followed by five washes with PBST (PBS, 0.05% Tween 20). One hundred µl/well of serial dilutions of CV-N mutant proteins (0.012–382 ng/well) in PBS was incubated with the *sgp120* plate for 1 h at room temperature. After five washes with PBST, CV-N mutant proteins bound to *sgp120* were detected with rabbit anti-CV-N polyclonal antiserum [1] at a 1/1000 final dilution, followed by three washes and incubation with secondary antibodies with horseradish peroxidase conjugate (Sigma, St. Louis, MO). The plate was then washed five times with PBST, following incubation with 100 µl of pre-warmed TMB substrate (Kirkegaard & Perry Laboratories, Gaithersburg, MD). After adding 50 µl of 2 M H₂SO₄, optical density was read at 450 nm.

Anti-HIV activity assay. The anti-HIV activity of the His-tagged proteins was characterized using the XTT-tetrazolium assay as described previously [20]. Briefly, 100 µl of serial dilutions of the cyanovirins was added to designated wells of a 96-well plate. Subsequently, CEM-SS cells at 1×10^5 cells/ml and HIV-1_{RF} virus were added in 50 µl quantities. Plates were incubated at 37 °C for seven days and stained with XTT. All values are averages of four replicates for protection and two replicates for toxicity and are represented as percentages of control.

Native-PAGE and SDS-PAGE. All the reagents used for native-PAGE and SDS-PAGE were from Invitrogen (Carlsbad, CA). For native-PAGE, samples (1 µg per lane) mixed with Tris-glycine native sample buffer were run on an 18% Tris-glycine gel with Tris-glycine native running buffer and the gel was stained by Coomassie blue. For SDS-PAGE, samples (1 µg per lane) mixed with tricine-SDS sample buffer containing 2% 2-mercaptoethanol were run on a 16% Tris-tricine gel with tricine-SDS running buffer and stained by Coomassie blue. Polypeptide SDS-PAGE molecular weight standards (Bio-Rad, Hercules, CA) were used.

Protein crystallization. Lyophilized P51S/S52P was dissolved in ultrapure water and used for crystallization. Screening of crystallization conditions [21] was carried out by the hanging drop, vapor-diffusion method [22], using the Hampton (Hampton Research, Laguna Niguel, CA) and Wizard (Emerald Biostructures, Bainbridge Island, WA) screens. Several conditions leading to crystal growth were identified in a very wide pH range, from 4.6 to 10.3. Diffraction-quality crystals were grown in 1.26 M ammonium sulfate and 0.1 M cacodylate, pH 6.5. The largest crystals grew in 10 days at room temperature to 0.5 mm × 0.4 mm × 0.4 mm. Before flash freezing, the crystals were transferred into a cryoprotectant solution consisting of 80% mother liquor and 20% ethylene glycol. A heavy atom derivative was obtained by soaking crystals for 2 h in a mother liquor also containing 10 mM PCMBs.

Crystallographic procedures. X-ray data for the P51S/S52P double mutant were collected on a Mar345 detector, using a Rigaku rotating anode X-ray source with CuK α radiation focused by an MSC/Osmic mirror system. Data were processed using the program Denzo and scaled using Scalepack [23] (Table 1). Molecular replacement was carried out with the program AMoRe [24], using a compact monomer of native CV-N as a search model. With the correct solution, the symmetry-related mates were generated; and while domain A was kept fixed, domain B was superimposed over the closest symmetry mate in

Table 1
Statistics of the crystallographic data

	P51S/S52P	
Ligand	–	PCMBS
Unit cell parameters	$a = b = 48.1$, $c = 79.67 \text{ \AA}$; $\alpha = \beta = 90^\circ$, $\gamma = 120.0^\circ$	$a = b = 47.69$, $c = 80.17 \text{ \AA}$; $\alpha = \beta = 90^\circ$, $\gamma = 120.0^\circ$
Space group	P3 ₂ 21	P3 ₂ 21
Molec/a.u.	1	1
Resolution (Å)	25–1.72	40–2.3
Total reflections	111,482	68,406
Unique reflections	11,809	4986
Completeness (%)	99.8	99.1
Avg. I/σ	43.4	107.4
R_{merge} (%)	4.7	5.2
Phasing power (20–2.3 Å)	–	0.95
R_{cullis}	–	0.83
$R_{\text{cullis,ano}}$	–	1.00

the linker region. The CNS [25] maximum-likelihood refinement procedure combined with simulated annealing [26] was used for structure refinement, with Engh and Huber geometric parameters [27]. The model was rebuilt into electron density using the program O [28]. The structure was refined to an R -factor of 25% and free- R [29] of 29.5%. To provide a model not dependent on molecular replacement, anomalous data were collected from a PCMBS derivative of CV-N and the positions of two Hg atoms were determined from a difference Fourier map. The metal positions were refined in MLPHARE [30], and after density modification with DM [30], the phases were used in WARP [31] for rebuilding the structure. This model was further modified in O and refined in CNS. The coordinates derived from molecular replacement have been submitted to the Protein Data Bank (PDB) with the accession code 1lom for immediate release.

Surface and volume analysis. Hydrogen atoms were added to the structural models using the builder module from InsightII (Accelrys, Burlington, MA) at their respective pH values, taking into account the lone pairs. PDB coordinates 3ezm were used for the low-pH model, while the set 115b was used to model the structure at high pH. The solution NMR structures 1j4v and 2ezm were used around neutral pH. The number of buried/surface atoms and surface charges was determined with DelPhi (Accelrys, Burlington, MA) using the CHARMM22 charge and atomic radii sets. The known ionic strength was used for each structure, with a solvent radius of 1.4 Å, zero boundary conditions, and a grid step of 1.5–1.6 Å/grid point. For structure superposition, the program ALIGN was used [32].

Results and discussion

Biological activity and the folding status of P51S/S52P

The CV-N mutant P51S/S52P, expressed in the periplasmic fraction of *E. coli* and purified as described in the Materials and methods, was used to evaluate the gp120-binding activity in an ELISA format, as well as the anti-HIV activity against a T-tropic laboratory strain (HIV-1_{RF}). The results showed that P51S/S52P exhibited essentially indistinguishable bioactivity characteristics compared to the wild-type CV-N (data not shown). We further studied the effects of the mutation on the protein folding of P51S/S52P, using the elec-

trophoretic mobility of the mutant CV-N on a native-polyacrylamide gel. Two bands which represent the monomer and the dimer were observed in both the P51S/S52P and wild-type CV-N sample. On the other hand, as reported elsewhere [17], S52P only migrated to about the same position as the dimeric form of wild-type CV-N and P51S/S52P, indicating that S52P existed only as a dimer (data not shown).

Overall structure of CV-N P51S/S52P

The structure of a monomeric form of CV-N was initially determined by NMR [10], whereas X-ray crystallography [9] revealed a domain-swapped dimer. A compact molecule of CV-N (or a half of the domain-swapped dimer) has an ellipsoidal shape. The two domains (A, consisting of residues 1–50 and B, comprising 51–101) are very similar in their primary and tertiary structures [9]. The two intramolecular, intradomain disulfide bonds (C8–C22, C58–C73) are important for maintaining the structural stability and for anti-HIV activity [8,33]. A trigonal crystal structure was solved from crystals grown at low pH in space group P3₂21 [9], whereas a tetragonal form was solved from crystals grown at high pH in space group P4₁2₁2 [34]. It is important to emphasize the conditions under which the crystals were grown, since depending on the crystallization conditions, an array of crystal forms belonging to different space groups can be obtained. In all crystal structures reported to date, CV-N is always seen in the dimeric, domain-swapped form. The overall fold of P51S/S52P (Fig. 1) is identical to the wild-type trigonal CV-N, with an r.m.s.d. of 0.29 Å between their pseudo-monomers (residues 1–47). However, there is a major difference in the linker region (residues 49–53)

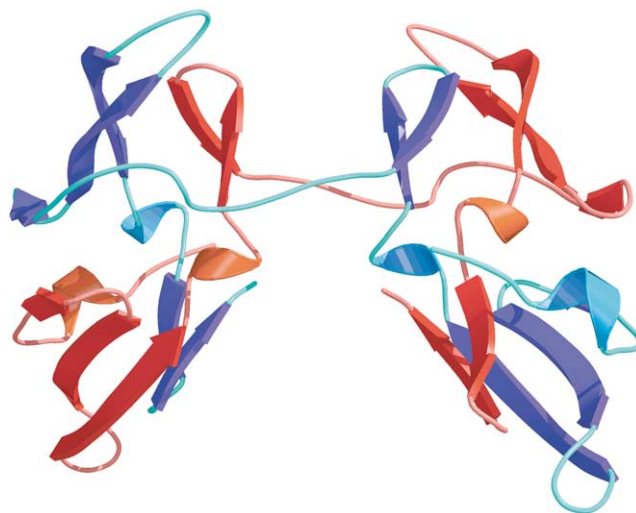


Fig. 1. The overall fold of P51S/S52P. Two domains (red and blue) are three-dimensionally domain swapped. This figure as well as the following ones are generated with the program MolScript [34].

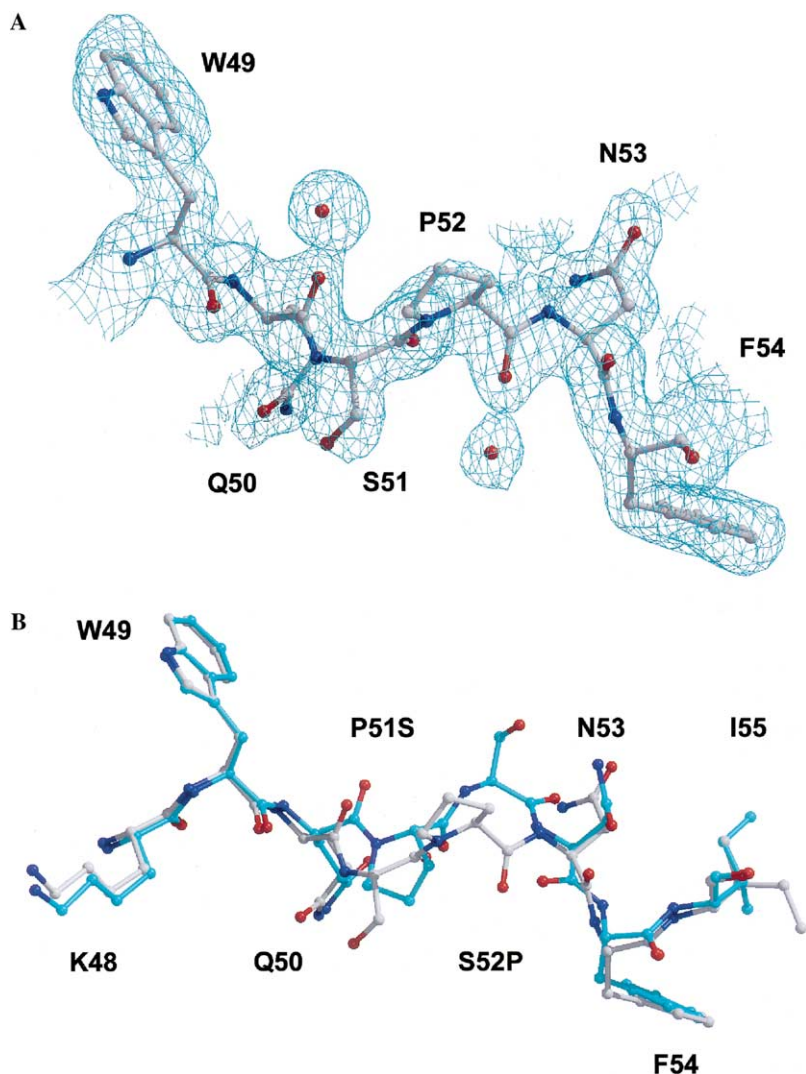


Fig. 2. A $2F_o - F_c$ electron density map of the P51S/S52P hinge region (A). Comparison of the linker region between the native CV-N (light blue) and the P51S/S52P mutant (B). Structures were aligned with the program ALIGN [32].

between the wild-type CV-N and the P51S/S52P mutant (Fig. 2).

Domain swapping

Two symmetrically related monomers (AB and A'B') form a dimer by three-dimensional domain swapping around the hinge region (residues 49–54). Domain A from one monomer interacts with domain B' from the other monomer and vice versa, forming two pseudo-monomers AB' and A'B. There is a range of orientations that the pseudo-monomers can adopt relative to each other in a domain-swapped dimer, depending on the experimental conditions. The significant change in the orientation of pseudo-monomers between low pH and high pH is illustrated in Fig. 3.

The results reported here challenge the previous hypothesis that domain swapping is the result of high protein concentration and low pH [9,14,15]. In our crystals

the protein concentration was fairly high (30 mg/ml), but the pH ranged from 4.6 to 10.3, proving that domain swapping is possible under a wider range of pH values, ionic strength, and organic solvent concentrations.

CV-N can exist in solution both in a monomeric and in a domain-swapped dimeric form, depending on the experimental conditions [18], whereas all the current crystal structures are exclusively domain-swapped dimers. The dimer is a metastable, kinetically trapped intermediate at neutral pH and room temperature; under such conditions, it can be stable for months [18]. At 38 °C, the metastable dimer converts into a thermodynamically more stable monomer in about 24 h.

Domain orientation

A comparison of CV-N structures under different pH conditions reveals a range of domain orientations (Fig. 3). The crystals of P51S/S52P are trigonal, despite the

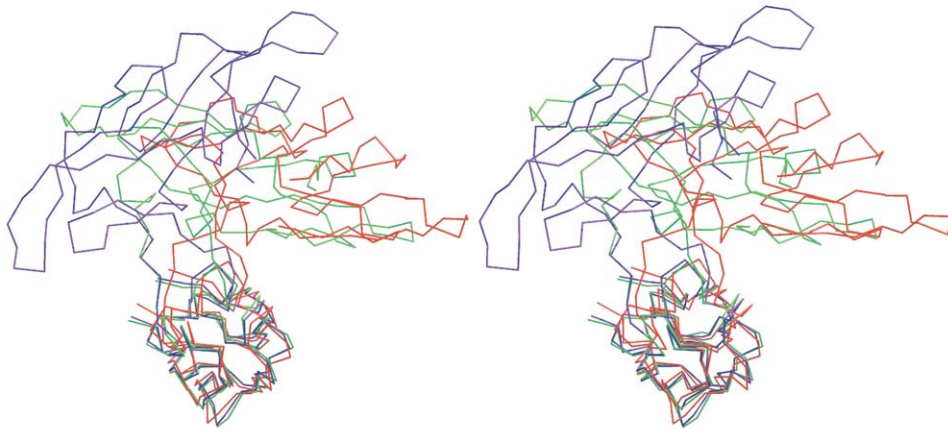
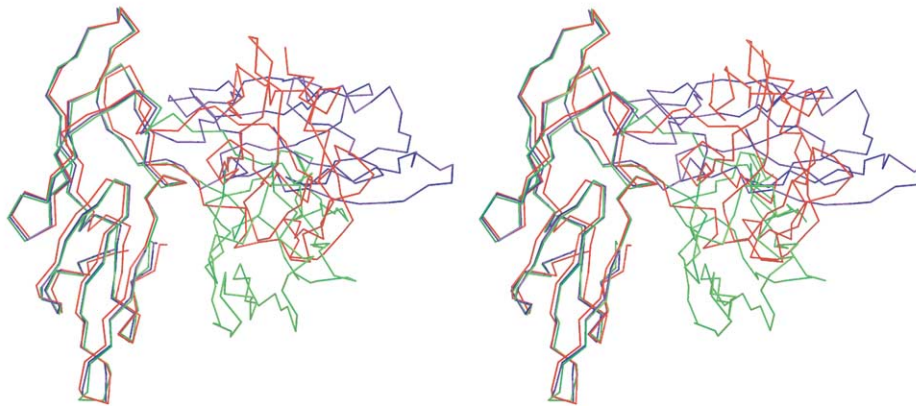
A**B**

Fig. 3. Stereo top (A) and side view (B) of pseudo-monomer orientation at different pH values. The same pseudo-monomer from the following structures was superimposed: low-pH crystal structure (blue), high-pH crystal structure (green), and pH 6.4 solution structure (red).

fact that they were grown at different pH values ranging from 4.6 to 10.3. Parallel refinement with AB monomer and AB' pseudo-monomer showed clearly a hinge region linking two domain-swapped monomers (Fig. 2A). However, the hinge regions between the domains run in a slightly different orientation than in the wild-type protein (Fig. 2B). For this mutant, the relative orientation of the two pseudo-monomers does not change as a function of pH. The question is raised again: what determines the relative orientation of the domains? Previous results emphasized the importance of the key proline residue in the hinge region in orienting the two domains [18]. This hypothesis can describe the current structures but is challenged by our results, since in the P51S/S52P structures, determined under a wide range of pH conditions, the domain orientation remains the same. It is unlikely that the two-residue swap in the mutant would yield a linker region so rigid that it could preserve the domain orientation, despite the change in pH. In our structure, the domains pack in a very similar way, re-

gardless of the pH or buffer conditions, and seem to determine the position of the whole hinge region. In an opposite scenario, where the hinge region determines the relative orientation of the domains, we would expect to see slightly different domain orientations, reflected by different crystal packing, or no crystal growth at all if the domain orientation would not allow proper packing.

The structure discussed here refines to a slightly high free-*R* (29.6%). Similar statistics were obtained for several independently collected and refined native data sets, raising the question of proper interpretation of the data initially dependent on molecular replacement. To remove any possibility that the high *R* factor was a result of model-induced bias, a mercury derivative data set was collected and the structure was determined again, independently of the native model. Although the presence of strong isomorphous and anomalous signals allowed the location of two mercury atoms bound to each CV-N molecule and led to acceptable phasing statistics, to no surprise this unbiased structure was virtually identical to

Table 2
Analysis of volume and buried surface area

	Wild-type CV-N	P51S/S52P	Wild-type CV-N	Wild-type CV-N	Wild-type CV-N
PDB code	3ezm	1lom	1j4v	115b	2ezm
Method	X-ray	X-ray	NMR	X-ray	NMR
Oligomer	Dimer	Dimer	Dimer	Dimer	Monomer
pH	4.4	6.0	6.4	10.3	7.0
Molecular volume (Å ³)	24493.4	24355.3	24705.1	24743.0	12248.8
Surface area (Å ²)	8642.2	8708.9	8533.1	9026.4	4457.9
Buried area	273.6	206.9	382.7	+101.6	–
Number of surface atoms	1119	1127	1141	1207	593
Number of buried atoms	2576	2548	2542	2490	1254
Total surface charge	1.06	–0.007	2.66	–3.36	3.48

the one obtained after molecular replacement. Since in both cases the final difference Fourier maps do not contain any significant peaks and the geometric parameters of the models are acceptable, the source of the somehow elevated *R* values has not been identified.

Surface and volume analysis

A comparative analysis of the molecular volume and surface area of the low pH and high pH dimers shows that there are significantly more atoms buried in the low-pH than in the high-pH structures (Table 2). The low-pH dimer is more compact, with a 250 Å³ smaller surface volume than the high-pH dimer. There are more buried atoms at low pH but it does not correlate directly with the buried area. The solution structure has more buried area than any of the crystal structures, suggesting that the CV-N molecules are more compact in solution and might be somewhat relaxed in the crystal lattice. This might be a direct consequence of crystal packing contacts, which supersede the interactions with the solvent and select for a homogeneous conformation of the molecule. In the high-pH crystal structure, the domains have looser packing, their positions creating additional volume and surface area in the hinge region between the pseudo-monomers. The number of surface/buried atoms correlates well with the increase in pH, suggesting that hydrophobic interactions might play an important role in the domain orientation.

Ions and buffer molecules

The high-pH tetragonal structure has a well-defined Na ion close to the hinge region, anchored by atoms OE1 of Gln50 from domain A and main-chain carbonyl O of Ser38 from domain B. This ion is not present in the low-pH trigonal structure and the P51S/S52P structure. In the P51S/S52P structure, there is a well-defined sulfate near the N-terminus, with a well-conserved position among structures at different pH values. These ions have a stabilizing effect on the respective regions, evident from a comparison of *B*-factors of corresponding resi-

dues from different crystal structures. In the high-pH structure, the *B*-factors for the N-terminal residues are higher than the average *B*-factor of the structure, whereas in P51S/S52P the N-terminus has average *B*-factors. Comparing the coordinates of the tetragonal, trigonal, and the double mutant structures, the largest differences are located around the carbohydrate-binding sites. Residues 1–3 show the second largest difference (r.m.s.d. = 0.52 Å) between trigonal and tetragonal forms but only 0.12 Å difference between trigonal native CV-N and the double mutant. This can also be attributed to the stabilizing effect of the conserved sulfate ion in the double mutant structures.

The P51S/S52P mutant has biochemical and biophysical characteristics equivalent to the wild-type CV-N and a structure which is significantly different in the hinge region. Some of the current hypotheses on domain swapping and on the role of hinge-region proline residues in domain orientation are challenged by the fact that this double-mutant crystallizes under a wide variety of conditions. The present structure contributes to the understanding of the relationship between hinge-region orientation and domain swapping in cyanovirins, permitting the structure-based design of domain-swapped CV-N mutants, perhaps with different anti-HIV activities.

Acknowledgments

We thank K.R. Gustafson, L.K. Pannell, R.C. Sowder II, J.B. McMahon, and R. Gardella for helpful discussions and technical support of this project. This work was supported in part by the Intramural AIDS Targeted Antiviral Program of the Office of the Director of the National Institutes of Health to A.W.

References

- [1] M.R. Boyd, K.R. Gustafson, J.B. McMahon, R.H. Shoemaker, B.R. O'Keefe, T. Mori, R.J. Gulakowski, L. Wu, M.I. Rivera, C.M. Laurencot, M.J. Currens, J.H. Cardellina, R.W. Buckheit Jr., P.L. Nara, L.K. Pannell, R.C. Sowder, L.E. Henderson, Discovery of cyanovirin-N, a novel human immunodeficiency virus-inactivating protein that binds viral surface envelope glyco-

- protein gp120: potential applications to microbicide development, *Antimicrob. Agents Chemother.* 41 (1997) 1521–1530.
- [2] E. De Clercq, Current lead natural products for the chemotherapy of human immunodeficiency virus (HIV) infection, *Med. Res. Rev.* 20 (2000) 323–349.
- [3] B. Dey, D.L. Lerner, P. Lusso, M.R. Boyd, J.H. Elder, E.A. Berger, Multiple antiviral activities of cyanovirin-N: blocking of human immunodeficiency virus type 1 gp120 interaction with CD4 and coreceptor and inhibition of diverse enveloped viruses, *J. Virol.* 74 (2000) 4562–4569.
- [4] M.T. Esser, T. Mori, I. Mondor, Q.J. Sattentau, B. Dey, E.A. Berger, M.R. Boyd, J.D. Lifson, Cyanovirin-N binds to gp120 to interfere with CD4-dependent human immunodeficiency virus type 1 virion binding, fusion, and infectivity but does not affect the CD4 binding site on gp120 or soluble CD4-induced conformational changes in gp120, *J. Virol.* 73 (1999) 4360–4371.
- [5] T. Mori, M.R. Boyd, Cyanovirin-N, a potent human immunodeficiency virus-inactivating protein, blocks both CD4-dependent and CD4-independent binding of soluble gp120 (sgp120) to target cells, inhibits sCD4-induced binding of sgp120 to cell-associated CXCR4, and dissociates bound sgp120 from target cells, *Antimicrob. Agents Chemother.* 45 (2001) 664–672.
- [6] A.J. Bolmstedt, B.R. O'Keefe, S.R. Shenoy, J.B. McMahon, M.R. Boyd, Cyanovirin-N defines a new class of antiviral agent targeting N-linked, high-mannose glycans in an oligosaccharide-specific manner, *Mol. Pharmacol.* 59 (2001) 949–954.
- [7] S.R. Shenoy, B.R. O'Keefe, A.J. Bolmstedt, L.K. Cartner, M.R. Boyd, Selective interactions of the human immunodeficiency virus-inactivating protein cyanovirin-N with high-mannose oligosaccharides on gp120 and other glycoproteins, *J. Pharmacol. Exp. Ther.* 297 (2001) 704–710.
- [8] T. Mori, R.H. Shoemaker, R.J. Gulakowski, B.L. Krepps, J.B. McMahon, K.R. Gustafson, L.K. Pannell, M.R. Boyd, Analysis of sequence requirements for biological activity of cyanovirin-N, a potent HIV (human immunodeficiency virus)-inactivating protein, *Biochem. Biophys. Res. Commun.* 238 (1997) 218–222.
- [9] F. Yang, C.A. Bewley, J.M. Louis, K.R. Gustafson, M.R. Boyd, A.M. Gronenborn, G.M. Clore, A. Wlodawer, Crystal structure of cyanovirin-N, a potent HIV-inactivating protein, shows unexpected domain swapping, *J. Mol. Biol.* 288 (1999) 403–412.
- [10] C.A. Bewley, K.R. Gustafson, M.R. Boyd, D.G. Covell, A. Bax, G.M. Clore, A.M. Gronenborn, Solution structure of cyanovirin-N, a potent HIV-inactivating protein, *Nat. Struct. Biol.* 5 (1998) 571–578.
- [11] M.P. Schlunegger, M.J. Bennett, D. Eisenberg, Oligomer formation by 3-D domain swapping: a model for protein assembly and misassembly, *Adv. Protein Chem.* 50 (1997) 61–122.
- [12] D. Xu, C.-J. Tsai, R. Nussinov, Mechanism and evolution of protein dimerization, *Protein Sci.* 7 (1998) 533–544.
- [13] M.J. Bennett, M.P. Schlunegger, D. Eisenberg, 3-D domain swapping: a mechanism for oligomer assembly, *Protein Sci.* 4 (1995) 2455–2468.
- [14] M.J. Bennett, D. Eisenberg, Refined structure of monomeric diphtheria toxin at 2.3 Å resolution, *Protein Sci.* 3 (1994) 1464–1475.
- [15] A.M. Crestfield, W.H. Stein, S. Moore, On the aggregation of bovine pancreatic ribonuclease, *Arch. Biochem. Biophys. Suppl.* 1 (1962) 217–222.
- [16] B.S. Kelley, L.C. Chang, C.A. Bewley, Engineering an obligate domain-swapped dimer of cyanovirin-N with enhanced anti-HIV activity, *J. Am. Chem. Soc.* 124 (2002) 3210–3211.
- [17] Z. Han, C. Xiong, T. Mori, M.R. Boyd, Discovery of a stable dimeric mutant of cyanovirin-N (CV-N) from a T7 phage-displayed CV-N mutant library, *Biochem. Biophys. Res. Commun.* 292 (2002) 1036–1043.
- [18] L.G. Barrientos, J.M. Louis, I. Botos, T. Mori, Z. Han, B.R. O'Keefe, M.R. Boyd, A. Wlodawer, A. Gronenborn, The domain-swapped dimer of cyanovirin-N is in a metastable folded state, Reconciliation of X-ray and NMR structures, *Structure* 10 (2002) 673–686.
- [19] T. Mori, K.R. Gustafson, L.K. Pannell, R.H. Shoemaker, L. Wu, J.B. McMahon, M.R. Boyd, Recombinant production of cyanovirin-N, a potent human immunodeficiency virus-inactivating protein derived from a cultured cyanobacterium, *Protein Expr. Purif.* 12 (1998) 151–158.
- [20] R.J. Gulakowski, J.B. McMahon, P.G. Staley, R.A. Moran, M.R. Boyd, A semiautomated multiparameter approach for anti-HIV drug screening, *J. Virol. Methods* 33 (1991) 87–100.
- [21] J. Jancarik, S.H. Kim, Sparse matrix sampling: a screening method for crystallization of proteins, *J. Appl. Cryst.* 21 (1991) 916–924.
- [22] A. McPherson, *Preparation and Analysis of Protein Crystals*, Wiley, New York, 1982.
- [23] Z. Otwinowski, *An Oscillation Data Processing Suite for Macromolecular Crystallography*, Yale University, New Haven, 1992.
- [24] J. Navaza, An automated package for molecular replacement, *Acta Crystallogr. A* 50 (1994) 157–163.
- [25] A.T. Brünger, P.D. Adams, G.M. Clore, W.L. DeLano, P. Gros, R.W. Grosse-Kunstleve, J.S. Jiang, J. Kuszewski, M. Nilges, N.S. Pannu, R.J. Read, L.M. Rice, T. Simonson, G.L. Warren, Crystallography and NMR system: a new software suite for macromolecular structure determination, *Acta Crystallogr. D* 54 (1998) 905–921.
- [26] A.T. Brünger, A. Krukowski, J.W. Erickson, Slow-cooling protocols for crystallographic refinement by simulated annealing, *Acta Crystallogr. A* 46 (1990) 585–593.
- [27] R. Engh, R. Huber, Accurate bond and angle parameters for X-ray protein-structure refinement, *Acta Crystallogr. A* 47 (1991) 392–400.
- [28] T.A. Jones, M. Kieldgaard, Electron-density map interpretation, *Methods Enzymol.* 277 (1997) 173–208.
- [29] A.T. Brünger, The free *R* value: a novel statistical quantity for assessing the accuracy of crystal structures, *Nature* 355 (1992) 472–474.
- [30] CCP4, Collaborative Computational Project, Number 4, 1994, The CCP4 suite: programs for protein crystallography, *Acta Crystallogr. D* 50 (1994) 760–763.
- [31] A. Perrakis, R. Morris, V.S. Lamzin, Automated protein model building combined with iterative structure refinement, *Nat. Struct. Biol.* 6 (1999) 458–463.
- [32] G.E. Cohen, ALIGN: a program to superimpose protein coordinates, accounting for insertions and deletions, *J. Appl. Crystallogr.* 30 (1997) 1160–1161.
- [33] K.R. Gustafson, R.C. Sowder, L.E. Henderson, J.H. Cardellina, J.B. McMahon, U. Rajamani, L.K. Pannell, M.R. Boyd, Isolation, primary sequence determination, and disulfide bond structure of cyanovirin-N, an anti-HIV (human immunodeficiency virus) protein from the cyanobacterium *Nostoc ellipsosporum*, *Biochem. Biophys. Res. Commun.* 238 (1997) 223–228.
- [34] R.M. Esnouf, Further additions to MolScript version 1.4, including reading and contouring of electron-density maps, *Acta Crystallogr. D* 55 (1999) 938–940.